



SRTTU

Journal of Computational and Applied Research
in Mechanical Engineering

jcarme.sru.ac.ir

JCARME

ISSN: 2228-7922

Research paper

Effect of shear state on fracture of refined grain pure copper

S. Khalilpourazary^a, M. Zadshakoyan^{a,*} and S. H. Hoseini^b

^aDepartment of Manufacturing and Production Engineering, Faculty of Mechanical Engineering, University of Tabriz, Tabriz, East Azarbayjan, Iran

^bFaculty of Mechanical Engineering, Urmia University of Technology, Urmia, West Azarbayjan, Iran

Article info:

Article history:

Received: 12/02/2019

Revised: 15/09/2019

Accepted: 19/09/2019

Online: 21/09/2019

Keywords:

Equal channel angular pressing,

Copper,

Lode angle,

Stress triaxiality.

*Corresponding author:

zadshakoyan@tabrizu.ac.ir

Abstract

In recent decades, the industrial applications of refined grained pure copper and its alloys have been expanded. The properties such as high strength, high density, and low deformability make these alloys more attractive. Hence, investigating the fracture mechanism of refined grained copper is of great significance. In this study, the fracture analysis of copper is investigated using the equal channel angular pressing process. Experimental results on metal alloys demonstrate that stress states should be incorporated in the constitutive equations. Therefore, the fracture process is analyzed by focusing on its relationship with the Lode angle variable. To prepare the equal channel angular processed specimens, a die set is manufactured, and tensile strength tests are carried out on dog-bone and notched flat plate specimens up to fracture. In addition, the mean value of grain sizes of the copper specimens is evaluated. The results demonstrate that the grain refining process profoundly enhances the load-carrying capacity of copper specimens. Moreover, the dog-bone tensile tests clearly show that the peak value of the strain hardening in refined grained copper occurs up to two passes, and after two passes the strain hardening drops. Furthermore, the results reveal that the Lode angle variable has a significant influence on the failure of the refined grained copper specimens.

1. Introduction

Copper is one of the non-magnetic metals which have good deformability, suitable corrosion resistant, high electrical conductivity, as well as high antibacterial properties [1]. Copper and its alloys are utilized in various mechanical components, including piston rings, bolts, shafts, aircraft hydraulic pressure lines, nuts, pipes, and many other applications. Hence, improving the

mechanical and metallurgical properties of copper is of great significance in metal forming processes. Severe plastic deformation (SPD) is recently used to augment the physical, mechanical, and metallurgical properties of metals [2]. Equal channel angular pressing (ECAP) is a severe plastic deformation method, which was first introduced by Segal [3]. During the grain refining process, metal samples undergo a simple shear deformation passing

through two channels with similar cross-sections. Two channels intersect at a certain angle called “channel angle”. The simple shear deformation occurs in the plane intersecting the crossing of the channels. Considerable refinement of the grain structure and an increase in the dislocation density of the material are the results of such deformation. The homogenous ultra-fine grained (UFG) microstructure obtained from the grain refining process impresses the physical property of the metal and increases hardness, and strength compared to the original coarse-grained (CG) status [4].

Since UFG metals with high strength, high density as well as low deformability have been developed. The fracture behavior of refined grain metals during their lifetime attracted more attention. Besterici et al. [5] studied the fracture behavior of the coarse and refined grain copper specimens with purity equal to 99.95% at ambient temperature. Dog-bone tensile samples of refined grain copper were fabricated and were forced to fail. The results demonstrate that the size of dimples and dispersion of them on the fracture surface reduces and increases up to the fourth ECAP pass, respectively. Kim et al. [6] investigated the failure process of copper with high purity via route C-ECAP process. The results confirmed that by raising the number of passes, shear stress is enhanced until the 8th-passes. Prior researches indicate that the stress triaxiality, the ratio of hydrostatic pressure to equivalent, which represent the effect of hydrostatic pressure in constitutive equations, has a significant influence on deformable material failure [7]. The effect of hydrostatic stress on deformable material failure was first investigated by Bridgman [8]. Hydrostatic stress increases the void generation, enlargement, and merging, which designates in literature as nucleation growth-coalescence of voids and speeds up the deformable material failure inception. High compressive/ tension pressures increase/decrease the deformability of metals than their deformability at atmospheric pressure [9]. Mc Clintock [10] analyzed the enlargement and merging of two voids having a cylindrical shape with perfect plastic behavior. The outcomes showed that the void growth directly depends on the hydrostatic pressure.

Besides the stress triaxiality, many scientists indicated that the Lode angle, which could be defined as a function of the second and third deviatoric stress invariants, also has an important effect on fracture process [11-13]. Bao and Wierzbicki [14] experimentally demonstrated that hydrostatic pressure is not the only variable governing the failure process of metals. Barsoum and Faleskog [15] presented the influence of the Lode angle variable on the failure process. Xue [16] introduced a phenomenological model to estimate the deformable material failure, which incorporates the influences of hydrostatic pressure and Lode angle variable. The Xue model is presented on the coordinate system, which is a function of pressure, Lode angle, and equivalent stresses. That model defines the influences of hydrostatic stress and Lode angle as a failure surface in the coordinate established by principal stress space.

According to the presented literature review, deformable material failure of the refined grain metals has not been studied in terms of the stress state. The central goal of this investigation is to consider this field of research by experimental considering the failure of coarse grain and refined grain copper with a purity of 99.7 %. A proper ECAP-die set is prepared to produce the refined grain copper specimens. The original diameter and length of the annealed copper specimens are chosen to be 30 mm and 120 mm, respectively. The dog-bone and notched flat plate samples of coarse and refined grain copper in the three successive passes are prepared. To compare the mechanical behavior of the coarse grain and refined grain copper specimens, tensile tests are performed on all machined ECAPed samples. Also, the microhardness values of all coarse and refined grain copper specimens up to three passes are investigated. Finally, the mean value of grain size of coarse grain and refined grain copper specimens are examined.

2. Governing equations

In this work, the effects of the stress state condition on the fracture type of the coarse grain and refined grain copper are investigated. Clausen studied the deformability variations in un-notched and plane strain tensile tests [17]. The results showed a remarkable decrease in

deformability of the notched flat plate samples of steel blocks compared to the un-notched axisymmetric ones. Xue claimed that the difference in deformability between these two cases is due to the change in the Lode angle variable, which varies between 0 to 1 [16]. To determine the integrated effect of the mean stress and Lode angle variable on the deformable fracture, a cylindrical coordinate system consists of the three invariants (p, θ, σ_{eq}) is employed, where p is the hydrostatic pressure, σ_{eq} is the von Mises equivalent stress, and θ is the Lode angle which is defined on the octahedral plane starting from a deviatoric axis (see Fig. 1.) [16]. The hydrostatic pressure, the von Mises equivalent stress, and Lode angle invariants can be formulated in a cylindrical coordinate system as follows [16]:

$$p = \frac{1}{3} tr \boldsymbol{\sigma} \tag{1}$$

$$\sigma_{eq} = \sqrt{\frac{3}{2} \mathbf{s} : \mathbf{s}} \tag{2}$$

$$\theta = \frac{1}{3} \arctan\left(\frac{3\sqrt{3} J_3}{2 J_2^{\frac{3}{2}}}\right) \tag{3}$$

where $\boldsymbol{\sigma}$, \mathbf{s} , J_2 , and J_3 are the Cauchy stress tensor, the deviatoric stress tensor, and the second and third invariants of the deviatoric stress tensor, respectively. In the plasticity and fracture, it is convenient to use the dimensionless hydrostatic pressure as the stress triaxiality parameter which is defined as [16]:

$$\eta = \frac{p}{\sigma_{eq}} \tag{4}$$

Similarly, the Lode angle can be normalized as follows [16]:

$$\bar{\theta} = 1 - \frac{|\pi - 6\theta|}{\pi} \tag{5}$$

Since the range of the Lode angle is $0 < \theta < \frac{\pi}{3}$, the range of the Lode angle variable is $0 < \bar{\theta} < 1$. According to Eqs. (4) and (5), all stress states can be considered by the stress triaxiality and Lode angle variables. Therefore, the stress state encountered in the conventional constitutive

models to estimate the fracture behavior by a set of parameters $\eta, \bar{\theta}$ [13, 14, 16].

In this research, the extension tests were done on the dog-bone and notched flat plate samples. Table 1 depicts the analytical terms for the stress triaxiality and the Lode angle variable parameter in dog-bone and notched flat plate samples.

3. Experimental method

Copper with a purity of 99.7% and without any atoms of oxygen was employed in this research. Table 2 presents the chemical composition of copper, based on BS EN 15079 standard [18]. The cylindrical shape annealed copper samples were machined with a radius and length of 15 mm 120 mm, respectively. Coarse grain copper specimens were annealed for 1 h at 550 °C and then cooled in the furnace. The grain refining process was implemented at ambient temperature using a split ECAP-die made of H13 steel with a channel angle of 90°. Route B_c was selected to carry out the grain refining process to get maximum mechanical and metallurgical properties [19]. In route B_c all specimens were revolved by 90° about the axial axis in the same direction between successive passes of the grain refining process.

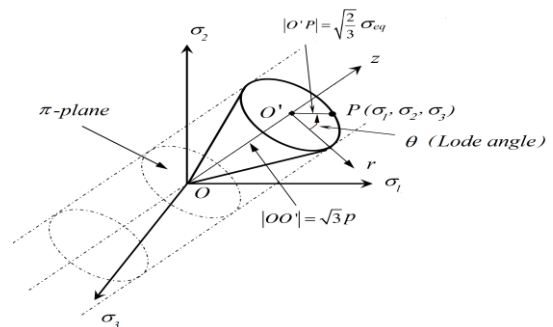


Fig. 1. A 3D representative of the stress state in the cylindrical coordinate systems [16].

Table 1. The values of stress triaxiality and the Lode angle variable in un-notched and notched flat plate tensile tests.

Specimen type	Analytical expressions for stress triaxiality	Lode angle variable
Dog-bone sample, tension	1/3	0
Notched flat plate, tension	$\frac{\sqrt{3}}{3} \left[1 + 2\ln\left(1 + \frac{t}{4R}\right) \right]$	1

R is the radius of a notch or a groove
t is the thickness of a notched flat plate

Table 2. The chemical composition of copper.

Element	Weight (%)
Cu	99.7
Fe	0.0407
S	0.0208
Pb	0.0383
Co	0.0139
P	0.0151
Others	0.1712

The split ECAP-die and the fabricated refined grain copper after the second pass are shown in Fig. 2.

To perform the grain refining process, the plunger velocity was selected 2 mm/s. In order to reduce the frictional force in intersected channels, molybdenum disulfide, (MoS₂) spray was employed. According to Eq. (1), the equivalent plastic strain magnitude for the first to third passes is 1.054, 2.10, and 3.16, respectively [1]:

$$\varepsilon = \left[\frac{n}{\sqrt{3}} \times \left[\frac{2}{\text{tg}(\frac{\phi}{2} + \frac{\psi}{2})} + \frac{\psi}{\sin(\frac{\phi}{2} + \frac{\psi}{2})} \right] \right] \quad (6)$$

where n is the number of passes, ϕ is die channel angle, ψ indicated the angle of the outer part of the die, and ε designates the plastic strain for each pass of the grain refining process. In this study, the angle of the outer part of the split ECAP-die was 20°. The manufactured coarse and refined copper specimens in 3 passes are shown in Fig. 3.

To specify the microhardness values Falcon 400 made by Innova Test Company with the force of 50 g and the dwell time of 10 s were employed based on ASTM E92 standard [20]. For each sample, the number of Vickers hardness was estimated six times random part of the surface; the values reflected in this research are the average of the measurements.

All of the coarse and refined copper tensile test samples were chosen from the center in the ECAP direction. Fig. 4 shows the position of the dog-bone and notched flat plate samples employed in the tensile tests.

The tensile test sample scheme with the dimensions in millimeters is presented in Fig. 5. The machining processes were performed on all dog-bone samples in Okuma CNC lathe machine

model Genos-L3000-E (Fig. 5(a)). Notched flat plate flat specimens were produced through the milling process in vertical machining center model VMC 8740 made by Lagun Corporation.



Fig. 2. ECAP-die and manufactured ECAPed copper.

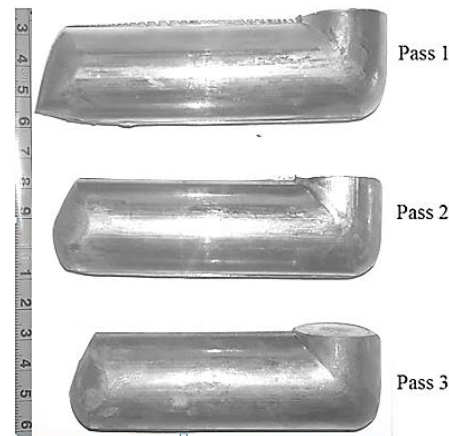


Fig. 3. Refined grain copper specimens in three passes (scale: centimeter).

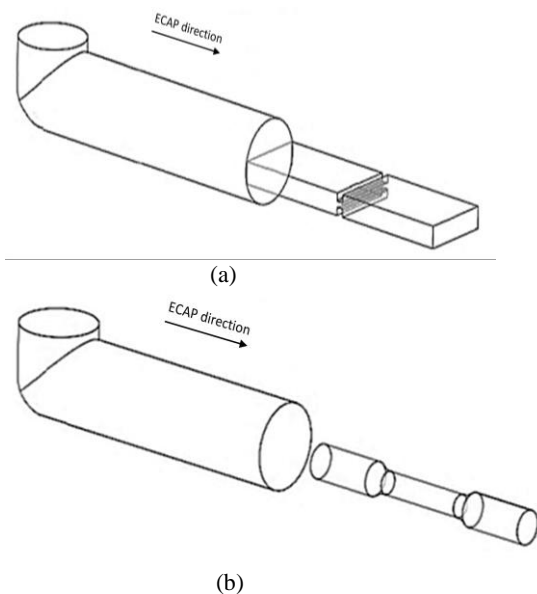


Fig. 4. The position of the tensile test samples; (a) notched flat plate and (b) dog-bone sample.

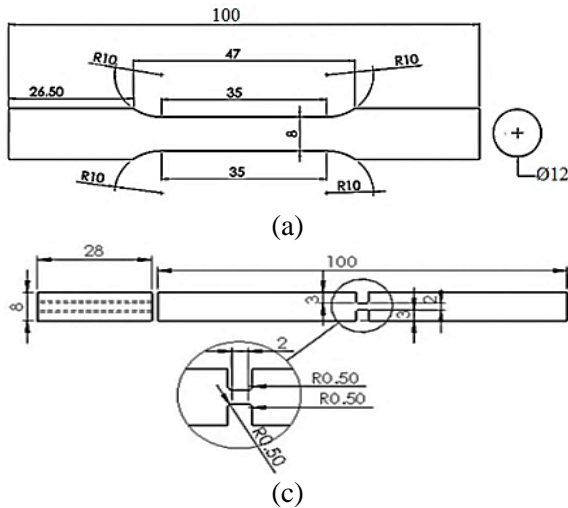


Fig. 5. Tensile test samples drawing (a) dog-bone sample and (b) notched flat plate.

After grinding the flat surfaces of the notched flat plate specimens, their bilateral grooves were manufactured in a wire EDM machine (Fig. 5(b)). The dimensions of the samples in the tensile test were selected according to the ASTM E8 standard [21]. All tensile test samples after the machining process are shown in Fig. 6.

Then, the samples were pulled up by 250KN-Santam materials testing machine (the Santam company model is STM 250) at ambient temperature until fracture happened. All samples were pulled thrice to guarantee the repeatability of results. All tensile tests were performed utilizing a constant rate of crosshead displacement with the nominal strain rate equal to 2×10^{-3} 1/s. The configuration of the notched flat plate specimen, in which its ends are fixed in the grippers, is presented in Fig. 7.

Also, an optical microscope model BA310MET manufactured by Motic Company, and the scanning electron microscope model MIRA3 FEG-SEM fabricated by Tescan Company with a voltage of 30 Kw were employed to investigate the structure of the annealed and refined grain copper specimens.

4. Results and discussion

The microstructures of coarse and refined copper specimens processed in first to third passes are presented in Fig. 8. Significant grain refinement happened during the grain refining process. The

mean value of the grain size of annealed copper equals 25 μm , while after three-passes of grain refining process, the mean value of grain size becomes 875 nm. The linear intercept technique was implemented to determine the mean value of grain size of the copper specimens, according to the ASTM E112 standard [22]. Xue et al. [23] reported that the refined grain copper has a mean value of grain size equals 305 ± 15 nm after six passes of the grain refining process.

Table 3 shows the mechanical properties of the coarse and refined grain copper specimens. As mentioned above, all samples were tested three times to guarantee the repeatability of the results. The average results of each test were presented in Table 3. Repeated experimental results show no significant discrepancy, and the deviation of the results is less than 3%.

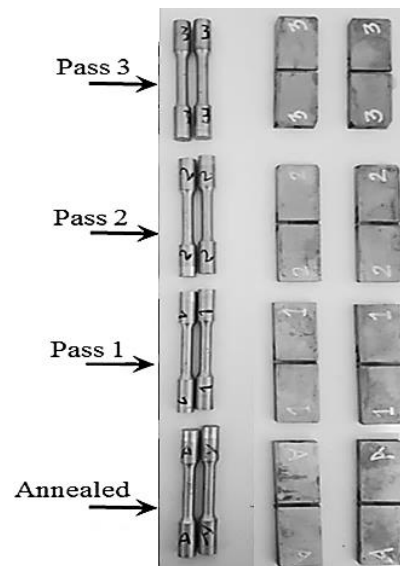


Fig. 6. Dog-bone and notched flat plate tensile test samples of coarse and refined grain copper.



Fig. 7. The configuration of the notched flat plate sample.

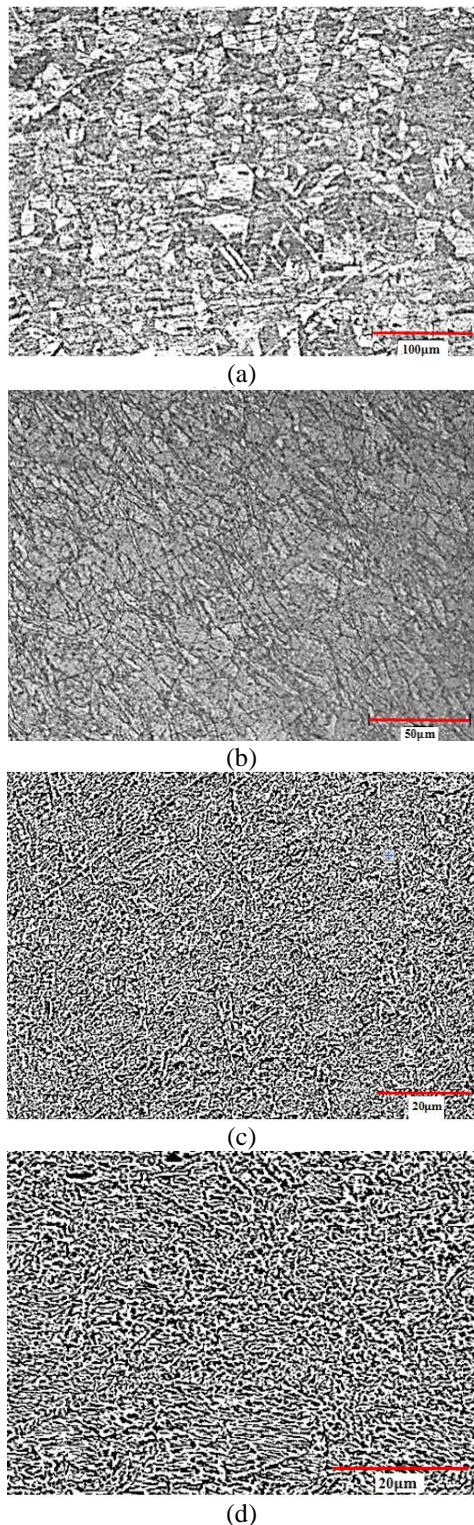


Fig. 8. Microtexture of copper with purity of 99.7%; (a) optical image of annealed copper, (b) optical image of one-pass, (c) SEM image of two-passes, and (d) SEM image of three-passes (etchant: 5g FeCl₃, 40 mL HCL, 100 mL ethanol).

The dog-bone sample force-displacement curves of the coarse and refined copper specimens in the three passes are displayed in Fig. 9. As regards the range of Lode angle variable $0 < \bar{\theta} < 1$, the Lode angle variable value in the dog-bone sample tensile test is equal to 0. Fig. 10 exhibits the engineering stress-strain curves of the coarse and refined grain copper after three passes. The results display that the grain refining process significantly improves the strength of refined grain copper samples. It is evident that the maximum value of yield strength in refined grain copper occurs after two-passes, and the dynamic recrystallization at ambient temperature initiates after three passes [24].

Table 3. Mechanical properties of all copper specimens in this research.

Number of passes	Annealed	1	2	3
Yield stress (MPa)	78	336	390	395
Vickers hardness number (HV)	71	126	134	142
Elongation (%)	54.5	22.38	19.5	15.8

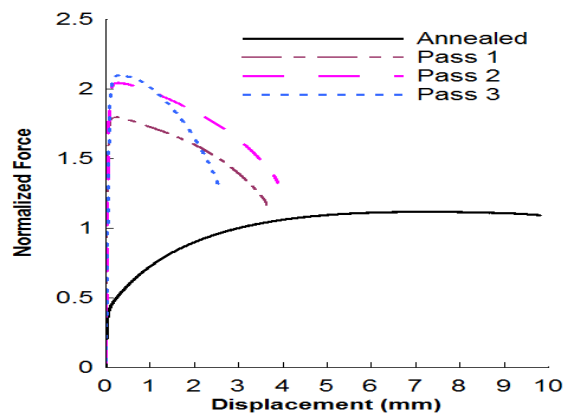


Fig. 9. Normalized force-displacement curves of the coarse and refined grain copper.

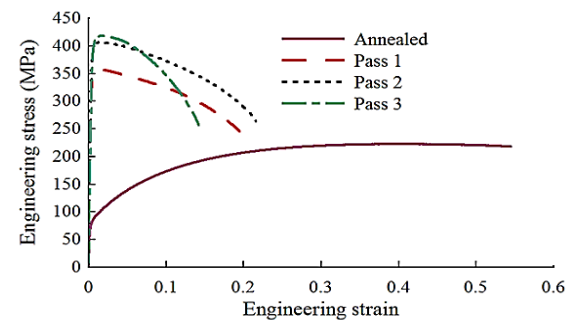


Fig. 10 Engineering stress-strain curves of copper specimens.

Due to the high defect density and grain refinement, the deformability of refined grain copper specimens during the grain refining process reduces. In other words, the combination of high hydrostatic pressure and large shear strains causes to increase the crystal lattice dislocation density, which can lead to significant refining of the grains [24]. According to Table 3, the annealed copper shows a large elongation to complete failure near 50%, but the elongation over all passes remains approximately constant near 20%. It is described by many scientists that the yield and ultimate tensile stresses reach their maximum values after four passes, and with repeating the processes the strength/the uniform elongation of the refined grain copper slightly decreases/ increases, respectively [25, 26]. This behavior can be related to the more uniform microstructure achieved after the three passes. After the second pass, the portion of the lamellar boundary structure with respect to the equiaxed subgrains is notably lower [25]. It also indicate the effect of the hydrostatic pressure on the failure process. In smooth specimens, after necking, the hydrostatic pressure of the stress state increases. As experimental results shows, hydrostatic pressure has a meaningful influence on increasing the strength and decreasing the deformability of refined grain copper.

A notched flat plate tensile test is employed to evaluate the material mechanical properties under shear conditions [16]. According to Fig. 5, the grooves are situated perpendicular to the longitudinal direction of the coarse and refined grain copper samples. During the tensile test, the fracture of the sample is taken place along the entire grooves. In the notched flat plate tensile test, the shear in the center region of the flat sample, as well as the hydrostatic pressure, indicates the stress condition [16].

Fig. 11 depicts the coarse and refined grain force via displacement contour of the notched flat plate specimens. The results exhibit the effect of the Lode angle variable on the deformable material fracture mechanism of the copper specimens. In the plane strain condition, the Lode angle variable reaches the maximum value indicating the shear dominant stress state. According to Fig. 11, the strength of refined grain copper specimens increases under plane strain conditions. It means that the grain refining

process as a severe plastic deformation technique increases the strength of copper under the shear dominant stress state. Moreover, the deformable material behavior of copper specimens during the grain refinement process gradually reduces. It is obvious that the influence of the Lode angle variable on the deformability reduction is less important than the effect of hydrostatic pressure.

The macroscopic presence of the fracture surface of dog-bone and notched flat specimens is shown in Fig. 12. The fracture type of the smooth annealed specimen is the classic cup-and-cone; however, the broken surfaces of the refined grain specimens show the slant fracture type. It means that the final failure of the refined grain copper specimens is a shear rupture with the fracture surface incline 45° to the loading direction.

The results prove the effectiveness of the microstructure texture on the deformable material fracture mechanism, which with the same stress state, the refined grain dog-bone specimens fractured with a different shape in comparison with the annealed one. As seen in Fig. 12(b), the fracture mode in all notched flat plate specimens is a slant fracture. Also, the angle of the surfaces with respect to the longitudinal direction of the specimens is exactly 45°. The slant fracture reflects that the fracture occurs under plane strain conditions, in which the Lode angle variable reaches unity. The results reveal the effect of the Lode angle variable on the deformable material failure process.

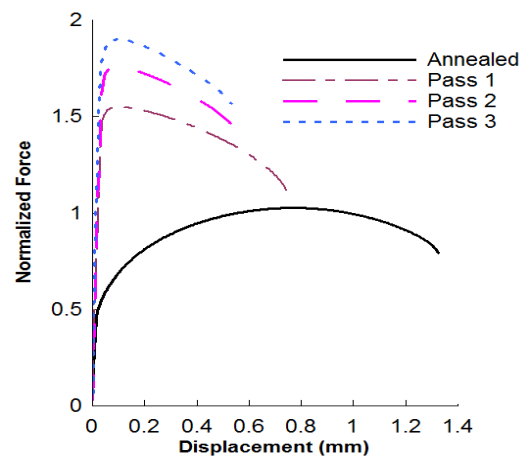


Fig. 11. Normalized force via displacement contours of the notched flat plate samples.

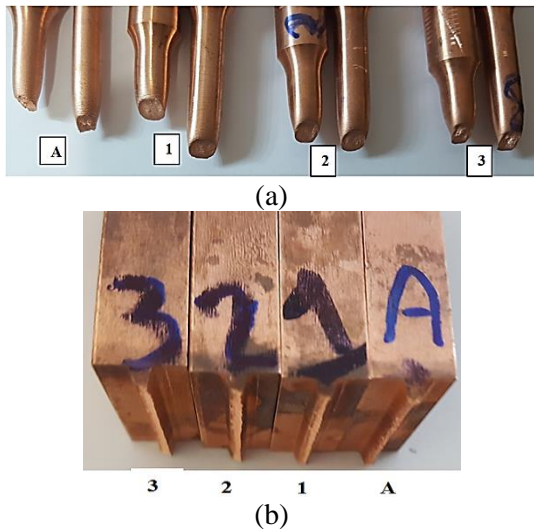


Fig. 12. Macroscopic appearance of (a) dog-bone samples: “A”: annealed, “1”: one-pass grain refining process, “2”: two-passes grain refining process, “3”: three-passes grain refining process, and (b) notched flat plate samples: “A”: annealed, “1”: one-pass grain refining process, “2”: two-passes grain refining process, “3”: three-passes grain refining process.

5. Conclusions

In this research, the deformable material failure of the coarse and refined grain copper specimens was investigated. A split ECAP-die was fabricated to prepare the refined grain copper specimens at room temperature. Then, the dog-bone and notched flat plate samples of the coarse and refined grain copper specimens in three passes were manufactured. To compare the mechanical behavior of the coarse and refined grain copper specimens, a series of tensile tests were implemented on all machined samples. Moreover, the mean value of grain sizes of the copper specimens was specified. Finally, the cross-section areas of fracture surfaces were scrutinized. Based on the obtained results, the important points can be summarized as follows:

- The grain refining process significantly improves the strength of copper components. After three passes, the yield strength of the copper improves by approximately 400%.
- The deformability of refined grain copper specimens during the grain refining operation remarkably reduces. After three passes, the elongation of the copper increases by approximately 270%.

- The load-carrying capacity of refined grain copper components also increases under plane strain conditions.
- The effect of the Lode angle variable on the deformability reduction is less than the effect of the hydrostatic pressure.
- The deformability of copper specimens during the grain refining process gradually decreases, and the Lode angle variable becomes one.
- With the same stress state, the fracture surface of the coarse grain dog-bone sample is the classic cup-and-cone type; however, the broken refined grain specimens exhibit the slant fracture.
- The angle of the fracture surface of notched flat specimens in the longitudinal direction of the specimen is 45°. The slant fracture of the notched flat plate specimens reveals that the fracture happens under a shear dominant state. For future research, it is beneficial to micromechanically investigate the shear dominant deformable material fracture in refined grain specimens such as aluminum, titanium, and steel.

References

- [1] J. R. Davis, *Copper and copper alloys*, ASM international, New York, pp. 10-102, (2001).
- [2] M. J. Zehetbauer and R. Z. Valiev, *Nanomaterials by severe plastic deformation*, John Wiley and Sons, Weinheim, pp. 50-126, (2006).
- [3] V. M. Segal, “Materials Processing by Simple Shear”, *Mater. Sci. Eng.: A.*, Vol. 197, No. 2, pp.157–164, (1995).
- [4] A. Rosochowski, *Severe plastic deformation technology*, Whittles publishing, Dunbeath, pp. 32-91, (2017).
- [5] M. Besterci, K. Sülleiová and T. Kvačkaj, “Fracture micromechanisms of Cu nanomaterials prepared by ECAP”, *Kovove Materialy*, Vol. 46, pp. 309-311, (2008).
- [6] Y.G. Kim, B. Hwang, S. Lee, C. W. Lee and D. H. Shin, “Dynamic deformation and fracture behavior of ultra-fine-grained pure copper fabricated by equal channel

- angular pressing”, *Mater. Sci. Eng.: A.*, Vol. 504, No. (1-2), pp. 163-168, (2009).
- [7] V. Tvergaard, “Material failure by void growth to coalescence”, *Adv. Appl. Mech.*, Vol. 27, pp. 83–151, (1989).
- [8] P. W. Bridgman, *Studies in large plastic flow and fracture*, McGraw-Hill, New York, pp. 121-134, (1952).
- [9] L. Xue, “Damage accumulation and fracture initiation in uncracked ductile solids subject to triaxial loading”, *Int. J. Solids Struct.*, Vol. 44, No. 16, pp. 5163-5181, (2007).
- [10] F. A. McClintock, “A criterion for ductile fracture by growth of holes”, *J. Appl. Mech.*, Vol. 35, pp. 363–371, (1968).
- [11] G. Z. Voyiadjis, S. H. Hoseini and G. H. Farrahi, “Effects of stress invariants and reverse loading on ductile fracture initiation”, *Int. J. Solids Struct.*, Vol. 49, No. 13, pp. 1541-1556, (2012).
- [12] R. Kiran and K. Khandelwal, “A triaxiality and Lode parameter dependent ductile fracture criterion”, *Eng. Fract. Mech.*, Vol. 128, pp. 121-138, (2014).
- [13] Y. Bai and T. Wierzbicki, “A new model of metal plasticity and fracture with pressure and Lode dependence”, *Int. J. Plast.*, Vol. 24, No. 6, pp. 1071–1096, (2008).
- [14] Y. Bao and T. Wierzbicki, “On fracture locus in the equivalent strain and stress triaxiality space”, *Int. J. Mech. Sci.*, Vol. 46, No. 1, pp. 81–98, (2004).
- [15] I. Barsoum and J. Faleskog, “Rupture mechanisms in combined tension and shear-experiments”, *Int. J. Solids Struct.*, Vol. 44, No. 6, pp. 1768–1786, (2007).
- [16] L. Xue, “Damage accumulation and fracture initiation in uncracked ductile solids subject to triaxial loading”, *Int. J. Solids Struct.*, Vol. 44, No. 16, pp. 5163-5181, (2007).
- [17] D. P. Clausing, “Effect of plastic strain state on ductility and toughness”, *Int. J. Fract. Mech.*, Vol. 6, No. 1, pp. 71-85, (1970).
- [18] ASTM BS EN 15079, *Copper and copper alloys: Analysis by spark optical emission spectrometry (S-OES)*, BSI Standards Publications, (2015).
- [19] M. Furukawa, Y. Iwahashi, Z. Horita, M. Nemoto and T. G. Langdon, “The shearing characteristics associated with equal-channel angular pressing”, *Mater. Sci. Eng.: A.*, Vol. 257, pp. 328-332, (1998).
- [20] ASTM E92-82, *Standard test method for Vickers hardness of metallic materials*, ASTM International, Philadelphia, (2003).
- [21] ASTM E8, *Standard test methods for tension testing of metallic materials*, ASTM International, Philadelphia, (2004).
- [22] ASTM E112–96, *Standard test methods for determining average grain size*, ASTM International, Philadelphia, (2004).
- [23] C. Xu, Q. Wang, M. Zheng, J. Li, M. Huang, Q. Jia, J. Zhu, L. Kunz and M. Buksa, “Fatigue behavior and damage characteristic of ultra-fine grain low-purity copper processed by equal-channel angular pressing (ECAP)”, *Mater. Sci. Eng.: A.*, Vol. 475, No. (1-2), pp. 249-56, (2008).
- [24] A. Mishra, B. K. Kad, F. Gregori and M. A. Meyers, “Microstructural evolution in copper subjected to severe plastic deformation: Experiments and analysis”, *Acta Materialia*, Vol. 55, No. 1, pp. 13-28, (2007).
- [25] M. Goto, S. Z. Han, J. Kitamura, T. Yakushiji, J. H. Ahn, S. S. Kim, M. Baba, T. Yaamoto and J. Lee, “S–N plots and related phenomena of ultrafine grained copper with different stages of microstructural evolution”, *Int. J. Fatigue*, Vol. 73, pp. 98–109, (2015).
- [26] F. Dalla Torre, R. Lapovok, J. Sandlin, P. F. Thomson, C. H. J. Davies and E.V. Pereloma, “Microstructures and properties of copper processed by equal channel angular extrusion for 1–16 passes”, *Acta Materialia*, Vol. 52, No. 16, pp. 4819–4832, (2004).

Copyrights ©2021 The author(s). This is an open access article distributed under the terms of the Creative Commons Attribution (CC BY 4.0), which permits unrestricted use, distribution, and reproduction in any medium, as long as the original authors and source are cited. No permission is required from the authors or the publishers.



How to cite this paper:

S. Khalilpourazary, M. Zadshakoyan and S. H. Hoseini, "Effect of shear state on fracture of refined grain pure copper," *J. Comput. Appl. Res. Mech. Eng.*, Vol. 11, No. 1, pp. 217-226, (2021).

DOI: 10.22061/JCARME.2019.4829.1589

URL: https://jcarme.sru.ac.ir/?_action=showPDF&article=1140

